UNIVERSITY OF BIRMINGHAM

Research at Birmingham

Air quality across a European hotspot

Masiol, Mauro; Squizzato, Stefania; Formenton, Gianni; Harrison, Roy; Agostinelli, A.

[Link to publication on Research at Birmingham portal](#)

AIR QUALITY ACROSS A EUROPEAN HOTSPOT: SPATIAL GRADIENTS, SEASONALITY, DIURNAL CYCLES AND TRENDS IN THE VENETO REGION, NE ITALY

Mauro Masiol[a,b,*], **Stefania Squizzato**[a,c], **Gianni Formenton**[d], **Roy M. Harrison**[b,§], **Claudio Agostinelli**[e]

[a] **Center for Air Resources Engineering and Science, Clarkson University, Box 5708, Potsdam, NY 13699-5708, United States**
[b] **Division of Environmental Health and Risk Management, School of Geography, Earth and Environmental Sciences, University of Birmingham, Edgbaston, Birmingham B15 2TT, United Kingdom**
[c] **Dipartimento Scienze Ambientali, Informatica e Statistica, Università Ca' Foscari Venezia, Campus Scientifico via Torino 155, 30170 Venezia, Italy**
[d] **Dipartimento Regionale Laboratori, Agenzia Regionale per la Prevenzione e Protezione Ambientale del Veneto, Via Lissa 6, 30174 Mestre, Italy**
[e] **Dipartimento di Matematica, Università degli Studi di Trento, via Sommarive 14, Povo, Trento, Italy**

[*] To whom correspondence should be addressed.
Email: mauro.masiol@gmail.com

[§] Also at: Department of Environmental Sciences / Center of Excellence in Environmental Studies, King Abdulaziz University, PO Box 80203, Jeddah, 21589, Saudi Arabia.

ABSTRACT

The Veneto region (NE Italy) lies in the eastern part of the Po Valley, a European hotspot for air pollution. Data for key air pollutants (CO, NO, NO_2, O_3, SO_2, PM_{10} and $PM_{2.5}$) measured over 7 years (2008/2014) across 43 sites in Veneto were processed to characterise their spatial and temporal patterns and assess the air quality. Nitrogen oxides, PM and ozone are critical pollutants frequently breaching the EC limit and target values. Intersite analysis demonstrates a widespread pollution across the region and shows that primary pollutants (nitrogen oxides, CO, PM) are significantly higher in cities and over the flat lands due to higher anthropogenic pressures. The spatial variation of air pollutants at rural sites was then mapped to depict the gradient of background pollution: nitrogen oxides are higher in the plain area due to the presence of strong diffuse anthropogenic sources, while ozone increases toward the mountains probably due to the higher levels of biogenic ozone-precursors and low NO emissions which are not sufficient to titrate out the photochemical O_3. Data-depth classification analysis revealed a poor categorization among urban, traffic and industrial sites: weather and urban planning factors may cause a general homogeneity of air pollution within cities driving this poor classification. Seasonal and diurnal cycles were investigated: the effect of primary sources in populated areas is evident throughout the region and drives similar patterns for most pollutants: road traffic appears the predominant potential source shaping the daily cycles. Trend analysis of experimental data reveals a general decrease of air pollution across the region, which agrees well with changes assessed by emission inventories. This study provides key information on air quality across NE Italy and highlights future research needs and possible developments of the regional monitoring network.

Keywords: air pollution, nitrogen oxides, particulate matter, Veneto, trends.

1.   INTRODUCTION

Since the mid-90s, the European Community has adopted increasingly stringent standards for abating emissions and for improving the air quality. The main steps in the legislative process were the Framework Directive 96/62/EC, its subsequent daughter Directives and the more recent Directive 2008/50/EC. As a consequence, a general improvement of air quality has been recorded in the last decade. However, current and future EU standards are still breached in some European regions, the so-called hotspots, e.g., Northern Italy, Benelux and some Eastern Countries (Putaud et al., 2004;2010). Under this scenario, the development of additional successful strategies for emission mitigation and the implementation of measures for air quality control are two major questions addressed by policy makers and in scientific research, respectively.

Following the implementation of the EC Directives, local and national authorities are required to monitor air quality. Measurement data are primarily managed by local agencies to assess the extent of air pollution, check if standards are complied with, and, in case of the exceeding of Limit Values or even lower assessment thresholds, to inform the population about potential health impacts. Beyond their original regulatory purpose, such data also represent a valuable resource: if historical data are available, long-term trends can be investigated to obtain real feedback upon the successes and failures of past and current mitigation strategies.

The Po Valley (N Italy) is neither a city nor an administrative unit, but it can be considered a megacity (Zhu et al., 2012). Currently, it is one of the few remaining and most worrying European hotspots: high levels of hazardous pollutants are commonly recorded over a wide area ($\sim 48 \cdot 10^3$ km^2) hosting ~16 million inhabitants. The anthropogenic pressure and some peculiar geomorphological features (a wide floodplain is enclosed by the Alps and Apennine mountains) lead to frequently breaches of limit and target values imposed by EU Directives (EEA, 2016) for nitrogen oxides, ozone and particulate matter (PM).

79   The Veneto Region (Figure 1) is located in the eastern part of the Po Valley and extends over

80   ~$18.4 \cdot 10^3$ km^2 ranging from high mountain environments (29% of the territory), to intermediate hill

81   zones (15%), large and flat plain areas (56%) and ~95 km-long coastlines. From an administrative

82   point of view, it is subdivided in 7 Provinces: Belluno (BL), Treviso (TV), Vicenza (VI), Venice

83   (VE), Padova (PD) and Rovigo (RO). Heavy anthropogenic pressures are present almost

84   continuously: a total of ~$4.9 \cdot 10^6$ inhabitants are resident in some large cities (>$2 \cdot 10^5$ inhabitants:

85   Verona, Padova and Venice-Mestre) and in a number of minor towns and villages which form a

86   continuum "sprinkled" network of urban settlements. Consequently, emissions from road traffic and

87   domestic heating are spread throughout the region. Some industrial areas are also present, mainly

88   close to the main cities and with distinctive features and different plant types. In addition, the

89   Veneto lies in a strategic location linking Central, Eastern Europe and continental Italy: a dense

90   network of international E-roads and transport hubs attract large amounts of road and intermodal

91   traffic, mostly heavy duty diesel-powered trucks. A large percentage of the region includes

92   agricultural fields, mostly located in the plain (intensive farming) and hilly areas (vineyards,

93   orchards), while rural environments are present mainly in hilly and mountain regions. A land use

94   map is provided in Figure 1: this composite landscape inevitably makes the emission scenario of the

95   region extremely complex and its spatial variations quite unpredictable.

96

97   This study aims to examine and describe the spatial variations, temporal trends and seasonality of

98   air quality across the Veneto Region over 7 years (2008-2014). Datasets used in this study include

99   the mass concentration of key air pollutants as required by European air quality standards: nitrogen

100   oxides ($NO+NO_2=NO_x$), ozone (O_3), carbon monoxide (CO), sulphur dioxide (SO_2) and PM with

101   aerodynamic diameter less than 10 µm (PM_{10}) and less than 2.5 µm ($PM_{2.5}$). Air quality data were

102   measured by ARPAV (Veneto Environmental Protection Agency) through a well-established

103   network of 43 sampling stations (ARPAV, 2014) covering a large portion of the territory (Figure 1).

104   A series of chemometric procedures are used to assess the extent of air pollution, to verify the

4

105 effectiveness of site categorization and to find patterns commonly recorded across the Veneto or

106 identify sites with anomalous pollution levels. The gradients of concentrations are depicted and

107 seasonal/diurnal/weekly patterns are investigated. The long-term trends are seasonally decomposed

108 and then processed to find the general orientations and drifts in air pollution over sites with a

109 different categorization. Furthermore, long-term trends are coupled with changes in the emission

110 inventories to verify if estimated emissions match with experimentally recorded levels of key air

111 pollutants across the region.

112

113 **2.   MATERIALS AND METHODS**

114 *2.1   Sampling sites*

115 The map of sites is shown in Figure 1, while Table 1 summarises their general characteristics and

116 measured pollutants. Figure 1 also shows the political, relief and land use maps. Sites are identified

117 by the initials for the province and their category. Sites were selected to fulfil some specifications:

118 (i) data availability must cover at least four years in 2008/14; (ii) sites must be representative of

119 most important pollution climate scenarios, such as citywide pollution, regional background or

120 traffic and industrial hotspots and (iii) sites must be representative of differing environments

121 (mountain, hilly, plain, coastal areas). In particular:

122 • At least one site was selected as rural background (RUR sites) for each Province (total 9 sites),

123   i.e. in areas not directly influenced by trafficked roads and/or urban and industrial settlements. In

124   particular, BL.RUR and VI.RUR are located in remote locations at high altitudes. RUR sites are

125   fundamental to assess the background gradients at the regional scale;

126 • Eighteen sites were categorised as suburban (SUB) and urban (URB), i.e. broadly representative

127   of citywide levels of air pollutants;

128 • A total of 8 sites were selected as representative of traffic hotspots (TRA) and placed at kerbside

129   locations in cities experiencing heavy traffic and/or frequent road congestion events;

130 • Eight sites were set as representative of main industrial (IND) areas. Each site has peculiar

131   characteristics. VE.IND is located downwind of Porto Marghera, one of the main industrial

132   zones in Italy extending over ~12 km^2 and including a large number of different installations

133   (thermoelectric power plants burning coal, gas and refuse derived fuels, a large shipbuilding

134   industry, an oil-refinery, municipal solid waste incinerators and many other chemical,

135   metallurgical and glass plants). VI.IND1 and VI.IND2 are representative of small and medium-

136   sized tannery industries, PD.IND1 and PD.IND2 are set in an area potentially affected by a

137   municipal solid waste incinerator plant, PD.IND3 was selected to monitor the fall-out from a

138   steel mill and VR.IND and PD.IND4 are representative of emissions from cement plants.

139

140 *2.2   Experimental*

141 All selected sites are equipped with fully automatic analysers set to collect data on hourly (gaseous

142 pollutants) or hourly/bihourly bases (PM_{10} and $PM_{2.5}$). QA/QC of measurements is guaranteed by

143 ARPAV internal protocols, which fully comply with the standards required by EC Directives in-

144 force: EN 14626:2012 for CO, EN 14211:2012 for NO, NO_2, and NO_x, EN 14212:2012 for SO_2,

145 EN 14625:2012 for O_3. CO, NO_x, O_3 and SO_2 instruments were calibrated every day. Hourly- or

146 bihourly- resolved PM_{10} and $PM_{2.5}$ were measured with beta gauge monitors: validation

147 experiments were routinely conducted between gravimetric (EN 14907:2005) and automatic

148 methods; several tests were also performed routinely (at least 1 test every week) to keep a constant

149 check on the beta gauge samplers. Pairs of filters were measured with both methods and the results

150 were checked to ensure that they are within the variation margins imposed by the technical

151 protocols adopted in UNI EN 12341:2001. Some sites were not equipped with hourly PM monitors

152 (Table 1), but may provide daily gravimetric-measured PM_{10} levels. In this case, PM was collected

153 by low-volume samplers on filters and the mass concentration was measured by gravimetric

154 determination (EN 14907:2005) at constant temperature (20±5°C) and relative humidity (RH,

155 50±5%). Consequently, no diurnal patterns are investigated in such sites, but only interannual and

156 seasonal trends.

157

2.3 QA/QC and data handling

159 Data have been validated by ARPAV through a well consolidated internal protocol (ARPAV, 2014)

160 and according to the European standards. The full dataset was therefore used for exploratory

161 statistics. However, the aim of this study is to detect the general behaviour of air pollution and some

162 clearly identified high pollution episodes which occurred in 2008/14 across the region. Examples

163 are the burning of a thousand folk fires on the eve of Epiphany (Masiol et al., 2014a) or fireworks

164 for Christmas and other local celebrations. Consequently, preliminary data handling and clean-up

165 are carried out to check the datasets for robustness, outliers and anomalous records. For this

166 purpose, data greater than the 99th percentile were included for exploratory analysis but not in the

167 trend estimation. Data were also adjusted to account for the shift in anthropogenic emissions due to

168 the changes between local time (UTC+1) and daylight savings time (DST). This latter correction

169 helps in investigating daily patterns of anthropogenic emission sources.

170

171 Data were analysed using R (R Core Team, 2016) and a series of supplementary packages,

172 including 'openair' (Carslaw and Ropkins, 2012; Carslaw, 2015), 'PMCMR' (Pohlert, 2015) and

173 'localdepth' (Agostinelli and Romanazzi, 2011;2013).

174

2.4 Data depth classification analysis

176 A classification analysis was used to check the accuracy of the site categorisation, i.e., to verify

177 whether the sampling sites in a category (RUR, SUB+URB, TRA, IND) are characterised by a

178 general homogeneity in air pollutant levels. This task is accomplished by applying a new

179 classification technique based on statistical data depth (DD). This technique is well reviewed

180 elsewhere (Mosler and Polyakova, 2012 and the reference therein) and recently was extended to

7

181   functional and multivariate data (Ramsay and Silverman, 2006; Lopez-Pintado and Romo, 2009;

182   Lopez-Pintado and Romo, 2011; Claeskens et al., 2014; Cuevas, 2014).

183

184   The depth of a point relative to a given dataset measures how deep the point lies in the data cloud,

185   i.e. it measures the centrality of a point with respect to an empirical distribution (Mosler and

186   Polyakova, 2012). DD provides an order to the observations and the rank system provided by DD

187   can be used to perform unsupervised and supervised classification analysis. A statistical depth

188   function should be invariant to all (non-singular) affine transformations; it reaches the maximum

189   value at the centre of symmetry for symmetric distribution and it becomes negligible when the norm

190   of the point tends to infinity. Another important property is ray-monotonicity, i.e. the statistical

191   depth does not increase along any ray from the centre (Liu, 1990; Zuo and Serfling, 2000). The

192   classical notion of data depth has been extended to functional data and the different available

193   implementations aim to describe the degree of centrality of curves with respect to an underlying

194   probability distribution or a sample. Some advisable properties of functional depths are the (semi-)

195   continuity, the consistency, and the invariance under some class of transformations, which tends to

196   vanish when the norm of a curve tends to infinity (Mosler and Polyakova, 2012).

197

198   A classification analysis was performed by using the DD-plot tool and a functional multivariate

199   simplicial depth. First, a (empirical) simplicial depth of a *point y* with respect to a *set of points x =*

200   *(x$_1$, ..., x$_n$)* in the Euclidean space of dimension p is introduced. $S_i = S(x_{i1}, x_{i2}, ..., x_{ip}, x_{ip+1})$ represents

201   the simplex obtained using *p+1* points in the sample. A simplex of *p+1* points in a space of

202   dimension p is the convex hull of those points. Then $d(y; x_n)$ is the fraction of simplicials S_n

203   contains y overall combinations of the *p+1* indices i_1, i_2, ..., i_p, i_{p+1} in the set *1,..., n*. This is a

204   consistent estimator of the simplicial depth, which is the probability that a random simplex $S(X_1, X_2,$

205    $..., X_p, X_{p+1})$ will cover the *point y* when $X_1, X_2, ..., X_p, X_{p+1}$ are identical and independent copies of

206   the random variable *X* from where the sample is drawn.

207   Thus, we can consider a set of (multivariate) curves $x_j(t)$, $(j=1, ..., J)$ measured at time $t_1, t_2, ..., t_N$,

208   i.e. $x_j(t_j)$ is a point in the Euclidean space of dimension p. In our context, $x_j(t)$ is the multivariate

209   time series at location j (sampling site) for a set of p pollutants concentration measured at time t.

210   Following Claeskens et al. (2014), we defined the depth of a given curve $y(t)$ according to the

211   sample $x=(x_1(t), ..., x_J(t))$, denoted $d(y(t), x)$ as the weighted average of the empirical simplicial

212   depth evaluated at any given time $t_1, t_2, ..., t_N$. The weights proportional to the fraction of available

213   observations at each time is then set. This is important to be considered for the presence of missing

214   values.

215

216   The classification is performed using the depth-versus-depth plot (DD-plot) (Li et al., 2012; Cuevas,

217   2014). Considering two groups of curves $x=(x_1(t), ..., x_J(t))$ and $z=(z_1(t), ..., z_K(t))$, the goal is to

218   classify a curve $y(t)$ in one of these. Hence, we evaluate $d(y(t),x)$ and $d(y(t),z)$ that represents the

219   depth of $y(t)$ according to x and to z. We assign $y(t)$ to the first group if $d(y(t),x) > d(y(t),z)$ and to

220   the second group otherwise. In particular, two groups of curves will be well separated if $d(x_j(t),x) >$

221    $d(x_j(t),z)$ for each observation x_j and $d(z_k(t),x) < d(z_k(t),z)$ for each observation z_k. Finally, we can

222   plot on a Cartesian axis the points $(d(x_j(t),x), d(x_j(t),z))$, $j=1,..., J$ and the points $(d(z_k(t),x),d(z_k(t),z))$,

223    $k=1,..., K$, i.e. the DD-plot. Curves (sampling sites) well classified in the first group will be plotted

224   at the right bottom corner of the graphics, whereas curves well classified in the second group will

225   appear at the left upper corner. Curves equally well classified in both groups will lie around the

226   bisector line of the plot.

227

228   In this study, four site categories are used to group the sites: rural (RUR), urban and sub-urban

229   (URB), traffic (TRA) and industrial (IND). For each couple of categories, the DD-plots are

230   evaluated on the basis of distributions of one or more pollutants.

231

232

3. RESULTS

A summary of data distributions during the whole study period (all available data) is provided as boxplots in Figure 2 and maps in Figures SI1. Concentrations are expressed as mass concentration; NO_x is expressed as NO_2, as required by EU standards. Moreover, Table SI2 reports annual average concentration and exceedances for NO_2, O_3, PM_{10} and $PM_{2.5}$. CO and SO2 are not included because no exceedances were observed.

3.1 *Carbon monoxide and sulphur dioxide*

In Veneto, CO and SO_2 are not critical pollutants. CO values are well below the EC limit value and WHO guidelines (WHO, 2000), i.e. 10 mg m^{-3} as daily maximum over eight hours. The highest hourly average levels of CO over six years were recorded at VR.URB1, PD.IND2, VR.TRA3, PD.URB, VE.TRA1 and PD.IND1 (all ~0.6 mg m^{-3}); remaining sites showed concentrations between 0.2 and 0.6 mg m^{-3}.

SO_2 does not show exceedances of European standards both for hourly averages (350 μg m^{-3}) and for 24-h averages (125 μg m^{-3}). The 2008/14 average concentrations across Veneto were very low, ranging from ~0.6 μg m^{-3} (often below instrumental detection limits) at VI.URB3 and RO.SUB to ~4 μg m^{-3} at some sites near Venice (VE.IND, VE.URB1). The higher levels in Venice sites can be likely associated to harbour and industrial emissions (i.e. thermal power plant, oil refinery and municipal solid waste incinerator). While the contribution of the harbour to the levels of SO_2 in Venice is still debated (Contini et al., 2015), the role of industrial emissions is well supported by the emission inventories. In 2005, about 76% of overall SO_2 emissions in the Veneto were released in the Province of Venice, of which 69% (19,742 Mg y^{-1}) came from combustion in energy and transformation industries (ARPAV, 2011).

3.2   Nitrogen oxides

When considering the short-term metrics, NO_2 does not represent a special risk for human health in Veneto: the 1-hour alert threshold of 400 μg m^{-3} was never breached, while the 1-hour average of 200 μg m^{-3} not to be exceeded more than 18 times over a calendar year was exceeded only at VR.TRA3 in 2008. However, NO_x becomes pollutants of concern when looking at the long-term metrics. The minimum average levels were found at two rural sites located in high mountain environments, while maxima were measured at a traffic site in Verona located very close to a logistic intermodal freight transport hub spanning over 4 km^2 and moving 26 million tons of goods annually (VR.TRA3). The average concentrations of NO varied from 0.5-0.6 μg m^{-3} (VI.RUR, BL.RUR1) to 50 μg m^{-3} (VR.TRA3), while NO_2 ranged from 4 μg m^{-3} (BL.RUR1) to 53 μg m^{-3} (VR.TRA3) and NO_x from 5 μg m^{-3} (BL.RUR1) to 130 μg m^{-3} (VR.TRA3). Comparing results averaged over 2008/14 with the annual EC limit value for NO_2 (40 μg m^{-3} averaged over one year), the limit was substantially exceeded at six traffic sites (VE.TRA2, VE.TRA1, VI.TRA, VR.TRA2, PD.TRA, VR.TRA3).

3.3   Ozone

In rural sites, average O_3 levels ranged from 48 μg m^{-3} (RO.RUR) to more than 90 μg m^{-3} (BL.RUR1, VI.RUR), while urban and suburban sites varied between ~40 and ~60 μg m^{-3}. Despite the low number of sites measuring ozone in traffic and industrial environments, it is evident that polluted environments generally exhibit the lower average concentrations: the minimum levels were recorded at VR.TRA3 (36 μg m^{-3}), which, inversely, shows the higher NO concentrations (it leads close to a large logistic intermodal freight transport hub and, thus, it is affected by heavy traffic of diesel-powered trucks).

Ozone is the subject of several regulations: the alert threshold (maximum 1-hour level of 240 μg m^{-3}) was never breached in 2008-2012, but was exceeded five times in 2013 at PD.RUR1. This

285 result recalls the anomaly of PD.RUR1 already reported for PM_{10}-bound polycyclic aromatic

286 hydrocarbons (Masiol et al., 2013). Despite PD.RUR1 being originally located far from direct

287 emission sources, it probably suffers from a local unknown source of air pollution. In addition, it is

288 located between and equidistant from three main urban settlements (Mestre, Padova and Treviso).

289 Further studies should be carried out to detect the potential sources; in the meanwhile, its

290 categorisation should be revised.

291

292 The information threshold (180 $\mu g\ m^{-3}$ over one hour) was frequently exceeded at most of the sites.

293 VI.RUR deserves special attention because it is affected annually by 39–126 exceedances; it is

294 located in a remote area (1366 m a.s.l.) characterised by grass- and wood-lands and is not affected

295 by direct anthropogenic sources. Consequently, high O_3 levels may be linked to the transport of air

296 masses containing ozone or ozone-precursors from the nearby highly populated plain areas or to the

297 local biogenic emission of ozone-precursors from plants. In addition, since this area is not impacted

298 by traffic, titration of photochemically produced ozone by primary NO is negligible.

299

300 The EC long-term target value of 120 $\mu g\ m^{-3}$ and the WHO air quality guideline of 100 $\mu g\ m^{-3}$

301 measured as maximum daily 8 hour running averages (not to be exceeded more than 25 days over 3

302 years for the EC target) were also frequently breached at almost all the sites. Similarly, the long

303 term objective value for the protection of vegetation (AOT40) calculated over the warm period

304 (May to July) is also amply breached at all the rural sites, posing a serious risk to high-quality

305 agriculture promoted by regional policies.

306

307 It is therefore evident that ozone is a critical pollutant across the Veneto. The standards for ozone

308 are more difficult to achieve across the warmer regions (southern Europe) because of the larger

309 magnitude of summer photochemical O_3 episodes. In addition, O_3 levels are also influenced

310 substantially by the extent of reactions with local NO emissions, which are currently falling in

311   Europe (Colette et al., 2011) in order to comply with the increasingly stringent emission standards

312   required for road vehicles. As a result, recent decreases in NO emissions across Europe may limit

313   reaction with O_3, which is the main sink of O_3 in the polluted atmosphere.

314

315   *3.4 NO_x partitioning and total oxidants (OX)*

316   Recent changes in emission trends for some air pollutants and the complex photochemistry of the

317   NO-NO_2-O_3 system are further evaluated through two derived parameters. The partitioning of

318   nitrogen oxides was investigated through the NO_2/NO_x ratio (Figure 2 and Figure SI1b) and total

319   oxidants ($OX=NO_2+O_3$, expressed as ppb) are often used to describe the oxidative potential (Kley et

320   al., 1999; Clapp and Jenkin, 2001). Results are highly variable, but higher ratios are generally

321   recorded at rural sites because of the lower primary NO emissions. The average levels of OX show

322   little variation across the Region with distributions typically showing interquartile ranges between

323   25 and 50 ppbv. The highest site averages are seen at rural sites due to photochemical ozone

324   creation, and at traffic sites, presumably caused by high emissions of primary NO_2.

325

326   *3.5   Particulate matter*

327   PM_{10} and $PM_{2.5}$ are critical air pollutants in Veneto. Average PM_{10} levels over 2008/14 varied from

328   less than 20 µg m^{-3} in BL.RUR2 and VR.RUR to more than 40 µg m^{-3} in VI.URB1 and VI.TRA.

329   Some sites breached the European annual limit value of 40 µg m^{-3} (PD.IND3, VI.URB1, PD.URB,

330   VR.TRA2, VE.TRA1, PD.TRA and PD.IND1), except in 2013 and 2014 when no exceedances

331   were recorded. In such sites, the annual average concentrations are usually close to the European

332   limit value: this way, small fluctuations in PM10 levels may have a large effect in marking them as

333   "fulfilling" or "not fulfilling" the EC standard. However, every year more than 20 sites exceeded

334   the daily mean of 50 µg m^{-3} for more than 35 times in a calendar year. Among these sites,

335   VI.URB1, VE.TRA2, VE.IND and VE.URB3 showed the highest number of daily exceedances for

336   a minimum of 77, 66, 64 and 60 times in a calendar year, respectively.

337

The $PM_{2.5}$ monitoring network started its operation in 2009, when the Directive 2008/50/EC entered

into force, and continued to grow over the following years. This way, only 8 sites provide sufficient

data to be included in this study. The annual limit value (25 µg m^{-3}) was frequently breached (five

years out of six) at PD.URB, PD.IND1, PD.IND2, VE.IND and VI.URB1. Similar to PM_{10}, in 2013

only 6 stations breached the annual average value, while no exceedances were recorded in 2014.

4.   DISCUSSION

4.1   Differences among sites

Maps showing the average levels of recorded pollutants over the 2008/14 period are reported in

Figures SI1a,b for different site categories. Levels of CO are generally low across the region and do

not show any evident trend among site categories. On the contrary, nitrogen oxides, SO_2, PM_{10} and

$PM_{2.5}$ show levels increasing from rural to urban to traffic sites, while concentrations in industrial

sites are highly variable and reflect the specific characteristics of each site (Figure 2). Such patterns

are opposite to ozone (higher levels at rural sites in high mountain environments and lower at sites

polluted with primary emissions).

Motor vehicles are major sources of NO (Keuken et al., 2012; Kurtenback et al., 2012) and a series

of volatile organic compounds (VOCs) (Gentner et al., 2013). Munir et al. (2012) have shown that

emissions from cars, buses and heavy vehicles have strong effects on urban decrements of ozone

levels. Due to this, the lower O_3 levels in most anthropogenically affected sites in Veneto are related

to the primary emissions of NO. This fact is further well supported by the partitioning of nitrogen

oxides (Figure SI1b): lower NO_2/NO_x ratios are recorded at urban and hot-spot sites, indicating that

high relative concentrations of NO lead to ozone depletion. Another reason is linked to the impact

of natural sources of VOCs, such as biogenic isoprene and terpenes, i.e. known effective ozone-

precursors (Duane et al., 2002). The land cover map (Figure 1) shows that the hilly and mountain

363 areas of N Veneto are covered by forests. Thus, biogenic VOCs are expected to be elevated in rural

364 and mountain environments and enhance the generation of ozone. In this context, modelling studies

365 in Europe indicate that biogenically-driven O_3 accounts for ~5% in the Mediterranean region (Curci

366 et al., 2009).

367

368 The Kruskal-Wallis analysis of variance by ranks (KW_{test}) was applied as a global non-parametric

369 test for depicting statistically significant inter-site variations. The null hypothesis is rejected for

370 $p<0.05$, meaning that the sites in a category are statistically different. In this case, the post-hoc test

371 after Nemenyi (Demšar, 2006) was applied for multiple sample comparison to point out the pairs of

372 sites which differ significantly in the pollutant level. Generally, results indicated that air pollutants

373 are uniformly distributed across the region: no pairs of sites differ in the levels of CO, while only

374 the two remote RUR sites (BL.RUR1 and VI.RUR) present statistically significant differences for

375 NO_x and ozone from a large number of other sites. The application of comparison tests for PM_{10} is

376 complicated by the lack of data at the two remote sites and by the availability of differently time

377 resolved data (hourly and daily). Despite such limitations, results indicate that only BL.RUR2

378 exhibits significantly lower concentrations than other sites.

379

380 *4.2   Differences amongst site categories*

381 KW tests indicated that the concentrations of many pollutants measured across the Veneto are

382 statistically similar even at sites which are categorised differently (except for the two sites located

383 in extremely remote mountain areas). Moreover, the results point to an important conclusion: air

384 pollutants are almost uniformly distributed across the region. However, these results also indicate

385 that there is an apparent homogeneity amongst sites, i.e. sites having different categorisation may

386 experience statistically similar levels of air pollutants. This hypothesis was tested statistically using

387 data depth (DD) analysis. However, there are some limitations to its application: the important

388 fraction of missing data for some pollutants/sites and the lack of the full set of pollutants at most

389 sites limits the possibilities for its use. Therefore, data-depth classifications were separately

390 performed for: NO, NO_2 and NO_x, (ii) PM_{10}, (iii) CO. Since few TRA and IND sites measured O_3

391 and SO_2, the DD analysis was not possible for these pollutants because not all the site categories

392 would be adequately represented. Application to one or a few pollutants has the disadvantage of

393 processing pollutants separately; however, it also has the advantage that it ensures the presence of a

394 reasonable high number of sites, which make the results more robust and the spatial extent of the

395 analysis more extensive.

396

397 The DD classification for nitrogen oxides (Figure 3) shows that most of RUR and URB sites are

398 generally well separated, i.e. they are plotted far from the 1:1 bisecting line. Rural sites are also well

399 separated from traffic and industrial ones. However, some exceptions are found. BL.SUB,

400 VI.URB3, VI.URB4 and RO.SUB are more similar to RUR than to URB sites, i.e. NO_x levels are

401 generally lower than other urban sites, as also confirmed by boxplots in Figure 2. On the contrary,

402 PD.RUR1 and RO.RUR lie on the URB-side of the DD plot, i.e. they are more comparable to URB

403 than RUR sites. Although the anomalously high levels of air pollution at PD.RUR1 were already

404 recognised and discussed (Masiol et al., 2013), this result also shows that two rural sites probably

405 experience relatively high levels of NO_x with respect to remaining RUR sites.

406

407 Although levels of pollutants in sites categorized as rural generally differ from other categories,

408 there is not a clear separation among URB, TRA and IND sites. In fact, the DD classification

409 analysis has demonstrated that most of the TRA and IND sites can be grouped with URB sites

410 (points lay around the bisector of the plot). DD-plots of PM_{10} also show this behaviour, while no

411 clear classification was possible using CO (Figure SI2 and SI3), i.e. CO levels are quite similar at

412 all site categories.

413

414 EU directives assume that URB sites are representative of the exposure of the general population,

415 while TRA and IND sites should be representative of areas where the highest concentrations may

416 occur. However, results show that this condition is rarely fulfilled in Veneto. In this context, a

417 recent position paper (JRC-AQUILA, 2013) has pointed out the need to implement criteria for

418 improving the classification and representativeness of air quality monitoring stations in Europe.

419 There are several reasons that may explain failure of the classification:

420 • The widespread distribution of emissions. Since the flat areas of the Po Valley host a 'sprinkled'

421   continuum of urban settlements with different sizes, densities and uses (Romano and Zullo,

422   2015), the rather constant presence of anthropogenic emissions leads to a widespread distribution

423   of emission sources. As a consequence, air pollutants emitted by different sources mix in the

424   atmosphere and the limited atmospheric circulation in Po Valley further limits their dispersion.

425 • The similarity of URB and TRA sites probably results from urban planning. Most large cities

426   have ancient origins and contain medieval or even Roman city centres with historic buildings

427   and narrow streets. A rapid and intense urbanization was experienced in Italy after World War II

428   with fast build-up of large urban/suburban areas all around the ancient city centres, often without

429   a well-informed approach to urban planning. Consequently, some city configurations

430   inevitability limit the movement of road traffic and are characterised by busy streets which are

431   frequently congested during rush hour periods, i.e. when traffic is widespread over the city

432   centres and not properly channelled into main orbital or bypass roads. The high density of

433   emissions leads to a high level of pollution from road traffic across cities and to the consequent

434   similar levels of pollutants between URB and TRA sites.

435 • The poor differentiation between URB and IND sites may result from the lack of large industrial

436   zones (except in VE). Most of Veneto cities host small and medium-sized industries in several

437   sectors: glass, cement, food products, wood and furniture, leather and footwear, textiles and

438   clothing, gold jewellery, chemistry, metal-mechanics and electronics. Large industrial zones are

439   only present in VE (Porto Marghera). In addition, during the last 20 years, a large number of

17

440   companies have relocated their plants abroad, while the global financial crisis (2007/9) has

441   overwhelmed the industrial and economic sectors with a consequent decrease in the production

442   of goods and/or the collapse, closure or downsizing of many companies/industries. Today,

443   small/medium sized industrial areas are scattered across the region, with many of the more

444   significant industries located close to major cities. As a result, some IND sites can be more

445   affected by urban sources than industrial emissions. For example, Porto Marghera, the main

446   industrial area of Veneto, lies SE of the city of Mestre. VE.IND (representative of Porto

447   Marghera) is located just east of the industrial area (Figure SI4). During winter frequent

448   temperature inversions are responsible for the build-up of air pollutants (mostly NO_x, PM) and

449   VE.IND lies just downwind of the urban area of Mestre under prevailing wind regimes (wind

450   rose in Figure SI4), while it is rarely downwind of the industrial area. Consequently, in winter

451   VE.IND is likely to be more affected by the plume from the urban area than by the industrial

452   emissions. This hypothesis is also confirmed by previous studies (Squizzato et al., 2014; Masiol

453   et al., 2012; 2014b), which reported similar concentrations of PM-bound species between

454   VE.IND and the city centre of Mestre. Further modelling studies are needed to inform

455   enhancements to the monitoring network and to better sample the industrial emissions.

456

457   *4.3   Spatial gradients*

458 The characteristics of anthropogenic pressures and the peculiar topography strongly influence the

459 pollutant distribution: this make the quantification of pollutant gradients very challenging. RUR

460 sites can be used as good estimators for determining gradients across the region because they can be

461 considered as representative of the regional pollution as suggested by Lenschow et al. (2001) for

462 PM: they are located away from large sources and are also fairly uniformly distributed across the

463 region. Average concentrations at RUR sites have therefore been spatially interpolated to

464 investigate the gradients of background levels of air pollutants across the region. Semi-variograms

465 were investigated, showing that all pollutants do not all have the same direction, and ordinary

466   kriging was selected as the best model to interpolate the data. In this study kriging analysis merely

467   aims to shape the background gradients because it was applied over a limited number of points (9).

468   Maps for pollutants recorded at more than six sites (NO_x, O_3, OX) are provided in Figure 4, while

469   the standard errors of predictions are shown in Figure SI5. All variables show marked gradients.

470   Nitrogen oxides increase from the mountain environments in the north to the coastal plain areas;

471   however the direction of maximum slopes in the increases differ slightly: NO from NW to SE,

472   while NO_2 is from NNW to SSE. The gradient for ozone is opposite to NO, with maximum

473   concentrations at high mountain rural sites and minima in coastal areas. The clear anti-correlation

474   between the gradients of NO and O_3 clearly depicts their relationship: at rural sites, NO emissions

475   from anthropogenic sources are low and therefore, the reaction with ozone is its main sink, and the

476   main sink for ozone. Due to the low concentrations of NO_2 at RUR sites when compared to ozone,

477   gradients for OX are similar to those of ozone.

478

479   ### *4.4   Seasonal patterns*

480   The monthly-resolved distributions of air pollutants are reported in Figure 5. No evident seasonal

481   patterns are found for the two high-mountain sites (BL.RUR1 ad VI.RUR). At the remaining sites,

482   all the pollutants except SO_2 exhibit clear seasonal cycles. CO, NO, NO_2, NO_x, PM_{10} and $PM_{2.5}$

483   show significantly higher levels in colder months (KW_{test} at $p<0.05$). Rapid increases occur between

484   mid-September and December; falls in concentration occur between March and mid-April. This

485   pattern can be attributed to the interplay of some covariant causes:

486   • The lower mixing layer heights in winter, which limit the dispersion of pollutants emitted

487   locally. The typical planetary boundary layer height in the Po Valley is 450 m in winter, and

488   rises up to 1500-2000 m in the warmer months due to the thermal convective activity (Di

489   Giuseppe et al., 2012; Bigi et al., 2012).

490   • Ambient temperature controls the gas-particulate phase partitioning of semivolatile compounds

491   (ammonium nitrate and part of organic carbon). In Veneto nitrate accounts for 0.1–0.5 $\mu g\ m^{-3}$

492 (0.7–2.5% of PM$_{2.5}$ mass) in August and for 5–10 µg m^{-3} (16–25%) in February (Masiol et al.,

493 2015) and organic carbon in PM$_{2.5}$ varies from about 2.6 µg m^{-3} in June and 11.4 µg m^{-3} in

494 December (Khan et al., 2016).

495 • Increased emissions in the coldest months mainly driven by increasing energy demand for

496 domestic heating. Domestic heating is regulated at national level: generally, the switching on is

497 fixed to occur on 15 October, while the switching off is on15 April, i.e. when the fastest changes

498 occur. However, such dates can change according to the weather. Wood smoke from domestic

499 heating may contribute appreciably to higher winter concentrations of PM.

500 • the drop of actinic fluxes in winter and the consequent reduction of hydroxyl radical, ozone, and

501 the oxidative activity which is a sink for many pollutants.

502

503 Ozone shows a strong seasonal pattern. Ozone shows the highest values during the warmest period

504 (generally Apr–Sep), when the solar radiation is higher (Figure 5) and the atmospheric

505 photochemistry is more active. Generally, ozone levels reach approx. 20 µg m^{-3} in winter, but never

506 drop below 50 µg m^{-3} at RUR sites located in high mountain environments (BL.RUR1, VI.RUR,

507 VR.RUR >800 m above sea level). The patterns of OX are dominated by ozone both in rural and

508 polluted sites: the highest levels were reached in the rural mountain sites (BL.RUR1 2020 m asl;

509 VI.RUR 1366 m asl and VR.RUR 824 m asl).

510

511 Sulphur dioxide lacks a clear seasonal pattern. Industrial emissions are expected to be quite constant

512 through the year, but highest emissions of SO$_2$ are may occur in summer due to an increase in

513 energy production from coal power plants to meet air conditioning demand. However, the higher

514 mixing layer height and the enhanced photochemistry driving S(IV) to S(VI) conversion lead to

515 similar concentrations to the cold period.

516

517

518

4.5   Daily and weekly patterns

Figure 6 reports the diurnal cycles, while Figure SI6 shows the weekly patterns. As for the seasonal

patterns, daily cycles are the result of interplays among the strength of sources, photochemical

processes and weather factors. Although minor changes due to peculiar local conditions are found,

almost all the sites exhibit rather similar daily and weekly cycles, except at the three high mountain

sites. CO and nitrogen oxides show typical daily cycles linked to road traffic at almost all the sites,

with two daily peaks corresponding to the morning and evening rush hours (7–9 am and 6–8 pm).

The morning and evening peaks are split by a minimum, which is assumed to be the result of: (i)

lower emissions (less traffic); (ii) larger availability of ozone driven by the daylight photolysis of

NO_x and the oxidation of VOC and CO (iii) higher convective activity leading to a deeper mixed

layer, which enhances the atmospheric mixing. Weekly patterns are also linked to road traffic:

generally, average levels increase from Mondays to Thursdays, while a fast drop is measured during

weekends, when road traffic reach minimum volumes and heavy duty vehicles over 7.5 tonnes are

subject to some limitations (over the whole weekends in summer and on Sundays in winter).

Ozone and total oxidants (OX) show evident daily peaks in the mid-afternoon, i.e. the hours

experiencing the higher solar irradiation, and lower levels are experienced between 6 and 9 am local

time (DST time-corrected in summer). These patterns are also enhanced in summer due to the

higher solar irradiation. It is evident that daily peaks of OX are delayed 2-3 hours with respect to

ozone, corresponding to the increased NO to NO_2 oxidation and primary NO_2 emissions in evening

rush hours. The weekly patterns are the mirror images of CO and NO_x with higher concentrations

during the weekends, following the drop of fresh anthropogenic emissions. However, such marked

diurnal patterns are not found at the three high mountain sites, which show rather constant and high

levels throughout the day. This "flatter" pattern has also been observed at other high-mountain sites

in the Apennines (Cristofanelli et al., 2007) and Alps (Vecchi and Valli, 1998) and is likely related

544   to the lack of anthropogenic sources of freshly emitted ozone-precursors and the presence of higher

545   levels of biogenic ozone-precursors, which do not follow anthropogenic cycling. However, the

546   levels of ozone in high mountain environments are also known to be strongly affected by (i) the

547   transport of polluted air masses by local wind systems (valley and slope winds) from the Po Valley

548   and surrounding cities inside the Alps (Kaiser et al., 2009), Foehn wind events (Seibert et al., 2000),

549   large scale synoptic air pollutant transport (Wotawa et al., 2000) and stratospheric inputs

550   (Vingarzan, 2004). Nocturnal dry deposition is also less effective at mountain sites.

551

552   Daily cycles of SO_2 are quite different thorough the region and between site categories and show

553   two different patterns. Most sites present NO_x-like patterns, i.e. two weak peaks corresponding to

554   the morning and evening rush hours. On the contrary, all RUR sites plus all sites in VE (with

555   different categorizations) and VI-URB3 (190 m a.s.l.) exhibited diurnal patterns very similar to

556   ozone, i.e. higher levels in the middle of the day. The two patterns remain different throughout the

557   year: different source emissions and weather factors may explain such patterns. The first cycle is

558   related to road traffic and is more evident at VR-TRA3 (close to a large logistic intermodal freight

559   transport hub), where the highest levels of NO_x are recorded. In Europe, sulphur content in

560   automotive gasoline and diesel is now limited to <10 ppm (since 2009), however it is clear that

561   large volumes in traffic and congestion during rush hours may have a key effect in shaping the

562   diurnal SO_2 levels. The second pattern was previously seen in Venice-Mestre (Masiol et al., 2014c)

563   and was related to local emissions from the nearby industrial zone hosting a large coal-fired power

564   plant and a large oil refinery, which are well known strong sources of SO_2, as indicated by local

565   emission inventories (ISPRA, 2015; ARPAV – Regione Veneto, 2015). The closeness of VE sites

566   to the sea drives the presence of sea/land breezes (mainly in warmest periods) and has a strong

567   influence of the local circulation pattern and in bringing air masses from the industrial zone to the

568   site locations. The daytime increase in SO_2 was also reported for a background site in London by

569   Bigi and Harrison (2010) who attributed it to the downward mixing of plumes from elevated point

570   sources as the boundary layer deepens during daylight hours.

571   Generally, PM_{10} exhibits higher concentrations overnight and clear minima in the early afternoon.

572   This pattern is consistent with the diurnal dynamics of the mixing layer. However, a secondary

573   cause may be related to the volatilisation of the more volatile aerosol compounds (e.g., nitrate)

574   during the early afternoon, i.e. when the air temperature is higher and relative humidity lower.

575   Minor peaks of PM_{10} concentrations can be found just before noon at a few sites affecting by very

576   different emission scenarios (VR.URB2, VR.URB3, VE.URB3, PD.RUR2, PD.IND4). Their

577   interpretation is not clear and may be related to the local characteristics of the sites.

578

579   *4.6   Long-term trends*

580   The long-term trends were analysed using the monthly-averaged data: since missing data can

581   significantly affect the trend analysis, only months having at least 75% of available records were

582   processed. In addition, only trends over periods extending more than 4 consecutive years were

583   computed. The quantification and the significance of the trends were evaluated by applying the

584   Theil-Sen nonparametric estimator of slope (Sen, 1968; Theil, 1992). This technique assumes linear

585   trends and is therefore useful to estimate the interannual trends, but it is irrespective of the shape of

586   trends. The slopes were also deseasonalized by using the seasonal trend decomposition using loess

587   (STL) to exclude the effect of the seasonal cycles. Details of STL are provided in Cleveland et al.

588   (1990). The statistics of the linear trends are listed in Table SI1 as percentage y^{-1}, while Figure SI7

589   shows all the single trends expressed in concentration y^{-1} along with the upper and lower 95th

590   confidence intervals in the trends and the *p*-values, which indicate the statistical significance of the

591   slope estimation.

592

593   The trends observed at each site reflect both regional and local changes and are affected by the

594   particular characteristics of the site locations. However, when trends observed at individual sites are

aggregated at provincial or regional levels, their relationships with current and past emissions inventories can be examined. The slopes calculated with the Theil-Sen method are then compared with changes in primary emissions as reported in various emission inventories (EIs) available at both regional and provincial level.

For each pollutant, statistically significant ($p<0.05$) trends expressed in percentage y^{-1} are provided in Figure 8 along with: (i) the differences in estimated emissions between 2010 and 2005 at provincial level provided by the EI SINAnet top-down (ISPRA, 2015) and (ii) the differences between 2010 and 2007/8 at regional scale provided by INEMAR (ARPAV – Regione Veneto, 2015). Differences of EIs (ΔEIs) are also expressed as percentage y^{-1} for an easier comparison with measured data (this choice considers a linear trend throughout the considered periods). Generally, most of the trends are negative for all the species and the changes in measured concentrations of CO, NO_x, PM_{10}, $PM_{2.5}$ agree well with EIs. However, some exceptions are also found (note that not all sites revealed statistically significant slopes).

CO concentrations decreased significantly at 12 of 18 sites with more than four years of available data, with slopes between -20.5% y^{-1} (TV.RUR) and -1% y^{-1} (PD.IND1). This result is in line with the average drops by -6.5% reported by INEMAR for the whole Veneto and with the EIs provided by SINAnet at province scale. However, some sites show the opposite behaviour, i.e. increased concentrations: BL.URB (+3.5% y^{-1}), VR.URB2 (+9.6% y^{-1}) and VE.TRA2 (+18.2% y^{-1}). Since falls of CO in EIs are mainly driven by road transport and non-industrial combustion (including biomass burning), such sites have possibly experienced local increases of road traffic volumes or emissions from the use of wood for domestic heating, which is widely used in mountain areas (mainly BL).

620   The average decrease of NO_x levels across the whole region was estimated as -4.1% y^{-1} by

621   INEMAR and was mainly attributed to "road transport" and, secondarily, to "combustion in energy

622   and transformation industry" and "combustion in industry" sectors. The average slope from data

623   measured experimentally at all the sites was -3.5% y^{-1}, ranging between -12.3% y^{-1} (VR.IND) and -

624   1.5% y^{-1} (VI.TRA). Statistically significant trends were negative at all sites except at VI.IND

625   (+1.5% y^{-1}). This result is a positive finding meaning that abatement strategies and improvement of

626   technologies had an effect in reducing the ambient levels of NO_x. However, in recent years there

627   has been increasing interest in NO_x emissions and NO/NO_2 partitioning in Europe. Evident

628   discrepancies have been found between achieving NO_x emission reductions and NO_2 ambient

629   concentrations, which do not meet the targets in many locations (e.g., Grice et al., 2009; Cyrys et

630   al., 2012). These concerns have been related to the recent increase in NO_2 levels in Europe due to

631   the increased proportion of diesel-powered vehicles, which are known to have higher primary

632   (direct) emissions of NO_2 (Carslaw et al., 2007). Since the recent boom of diesel vehicles was also

633   experienced in Italy (Cames and Helmers, 2013), the relationship between significant trends of NO_x

634   and NO_2 needs to be further investigated.

635

636   Analysis of trends in SO_2 requires particular care. Based on EIs estimations, a significant drop (-

637   14% y^{-1}) was experienced across the whole region, while at province level SO_2 emissions decreased

638   between -18% y^{-1} (in RO) and -6% y^{-1} (in BL). These drops in EIs are principally attributed to the

639   sector of combustion in energy transformation industries. In Veneto, this sector is mostly

640   represented by the energy production in coal-fired power stations, which is present in VE province

641   (Porto Marghera). In addition, the sector of 'other mobile sources' has also experienced significant

642   drops, particularly of ship emissions (present only in coastal areas of VE province): from January

643   2010, ships in the harbours are requested to use fuels with sulphur content <0.1%. According to the

644   EIs, experimental data show that all sites in the VE province and PD.IND2 have negative trends,

645   while four sites have experienced statistically significant increases in SO_2 levels, i.e. VI.URB3

646   (+24.5% y^{-1}), VR.RUR (+11.4% y^{-1}), PD.TRA (+9.9% y^{-1}) and RO.TRA (+7.4% y^{-1}). While the

647   decline at VE sites may be attributed to the concurrent fall in industrial and maritime source

648   emissions at a local scale, the increases at other sites deserve further investigation and are possibly

649   due to long-range transport of polluted air masses. In this context, a recent study (Masiol et al.,

650   2015) has reported that Eastern Europe is a potential source area for $PM_{2.5}$-bound sulphate, i.e. the

651   major sink for atmospheric SO_2.

652

653   Measured data fit well with changes in EIs for PM_{10}, except in VI province. All statistically

654   significant trends calculated from field data show decreases in PM_{10} concentration ranging between

655   -5.6% y^{-1} in BL.RUR2 and -1.9% y^{-1} in RO.TRA. PM_{10} emissions estimated by EIs dropped

656   between -4.4% y^{-1} in RO province and -2.4% y^{-1} in VR, with a slight increase in VI (+1.1% y^{-1}). At

657   a regional scale, the INEMAR inventory reports an overall decrease of -5.7% y^{-1}. Results for $PM_{2.5}$

658   are quite variable, mostly due to the short series of available experimental data: only 3 sites present

659   more than 4 years of data, of which only 2 have statistically significant trends. Hence, no further

660   information can be extracted for $PM_{2.5}$.

661

662   **Conclusions**

663   Air quality data from 43 monitoring sites have been used as input for a number of statistical tools to

664   assess the extent of air pollution across the Veneto. This paper is the first one providing information

665   from a large number of sites over a wide region of N Italy. The main findings can be summarised as

666   follows:

667   • Carbon monoxide and sulphur dioxide show low levels across the region and, therefore, are not

668   considered as critical pollutants. While CO does not show any evident spatial trend, SO_2 levels

669   are higher in VE Province, particularly around Venice-Mestre. This anomaly was linked to the

670   industrial zone (coal power plant, oil refineries, other industrial installations) and harbour

671   activities;

- Nitrogen dioxide, ozone and particulate matter (both PM_{10} and $PM_{2.5}$) are critical pollutants in view of protecting human health, i.e. the EC limit and target values are frequently breached at some sites. Those air pollutants deserve special attention because of their known adverse effects upon public health: future mitigation strategies should focus on reducing concentrations of such key pollutants;

- Air pollutants are quite uniformly distributed across the region: no pairs of sites have statistically significant differences in the levels of CO, while only the two remote rural sites present statistically significant differences from a large number of other sites for NO_x and ozone;

- The current site categorization was tested by applying a data depth classification analysis: results show that sites categorized as rural generally differ from other categories, while there is not a clear separation among urban background, traffic and industrial sites. Probable causes of the poor classification are discussed; some insights for improving the monitoring network are provided;

- Spatial trends were investigated by interpolating average concentrations at the rural sites: despite NO and NO_2 having a slightly different direction of maximum slopes, nitrogen oxides generally increase from the mountain to the coastal plain environments, while ozone presents maxima concentrations at high mountain rural sites and minima in coastal areas;

- Seasonal pattern analysis revealed that CO, NO, NO_2, NO_x, PM_{10} and $PM_{2.5}$ show significantly higher levels in colder months and minima in summer. This pattern is mainly attributed to the lower mixing layer heights, the limited oxidation potential and the emissions from domestic heating. The volatilization of semi-volatile aerosol compounds during the warmer seasons is another reason of this behavior for PM. On the contrary, ozone has an opposite seasonality with maxima in summer due to its increased photochemical generation. No seasonal patterns are found for SO_2;

- Diurnal and weekly cycles were investigated. Generally, similar patterns are observed across the region for all the measured species. A strong potential effect of road traffic emissions was found

698   for CO and nitrogen oxides: one/two daily peaks are commonly found at urban and hotspot sites

699   and were related road traffic emissions during rush hours. Ozone cycles were shaped by the

700   photochemistry and by the interplay with NO. PM cycles generally show higher levels overnight

701   and , therefore, are mostly shaped by the mixing layer height dynamics;

702   •   An overall decrease of all measured species (except ozone) was observed throughout the region.

703   Generally, results of trend analysis well fit with changes in emission inventories. However,

704   some sites with opposite trends have been identified; the reasons for increasing concentrations

705   in such sites needs to be further investigated.

706

707   **Disclaimer**

708   The views and conclusions expressed in this paper are exclusively of the authors and may not reflect

709   those of ARPAV.

710

714

715   **REFERENCES**

716 Agostinelli, C. Romanazzi, M. Local depth. J. Stat. Plan. Inference 2011;141(2):817-830.
717 Agostinelli, C. Romanazzi, M. Nonparametric analysis of directional data based on data depth. Environ Ecol Stat 2013;
718   20(2):253-270.
719 ARPAV (Environmental Protection Agency of Veneto Region).). Relazione Regionale Qualità dell'aria – Anno 2011
720   [in Italian], 2012. Available from: http://www.arpa.veneto.it/temi-
721   ambientali/aria/riferimenti/documenti/documenti-1 (last accessed: June 2015).
722 ARPAV(Environmental Protection Agency of Veneto Region). Relazione Regionale Qualità dell'aria – Anno 2013;
723   2014 [in Italian]. Available from: http://www.arpa.veneto.it/temi-
724   ambientali/aria/riferimenti/documenti/documenti-1 (last accessed: June 2015).
725 ARPAV (Environmental Protection Agency of Veneto Region) – Regione Veneto. INEMAR VENETO 2010 -
726   Inventario Regionale delle Emissioni in Atmosfera in Regione Veneto, edizione 2010 – Risultati
727   dell'edizione 2010 in versione definitiva – Relazione generale. ARPA Veneto - Osservatorio Regionale Aria,
728   Regione del Veneto - Dipartimento Ambiente, Sezione Tutela Ambiente, Settore Tutela Atmosfera; 2015 [in
729   Italian]. Available at: http://www.arpa.veneto.it/temi-ambientali/aria/emissioni-di-inquinanti/inventario-
730   emissioni [last accessed on Nov 2015]
731 Anttila P, Tuovinen JP, Niemi JV. Primary NO2 emissions and their role in the development of NO2 concentrations in a
732   traffic environment. Atmos Environ 2011;45(4):986-992.
733 Bigi A, Harrison RM. Analysis of the air pollution climate at a central urban background site, Atmos Environ 2010; 44:
734   2004-2012.

735 Bigi A, Ghermandi G, Harrison RM. Analysis of the air pollution climate at a background site in the Po valley. J
736   Environ Monit 2012;14:552-563.
737 Cames, M., Helmers, E. Critical evaluation of the European diesel car boom—global comparison, environmental effects
738   and various national strategies. Environ. Sci. Europe 2013;25(1):1.
739 Carslaw DC. The openair manual — open-source tools for analysing air pollution data. Manual for version 28th January
740   2015, King's College London; 2015.
741 Carslaw DC, Ropkins K. openair - an R package for air quality data analysis. Environ Model Softw 2012;27-28:52-61.
742 Claeskens G, Hubert M, Slaets L, Vakili K. Multivariate functional halfspace depth. J Am Stat Assoc 2014;
743   109(505):411–423.
744 Clapp, L.J., Jenkin, M.E. Analysis of the relationship between ambient levels of O3, NO2 and NO as a function of NOx
745   in the UK. Atmos. Environ. 2001;35:6391–6405.
746 Cleveland RB, ClevelandWS,McRae JE, Terpenning I. STL: a seasonal-trend decomposition procedure based on loess.
747   J Off Stat 1990;6(1):3–73.
748 Colette A, Granier C, Hodnebrog Ø, Jakobs H, Maurizi A, Nyiri A, et al. Air quality trends in Europe over the past
749   decade: a first multi-model assessment. Atmos Chem Phys 2011;11(22):11657-11678.
750 Contini D, Gambaro A, Donateo A, Cescon P, Cesari D, Merico E, Citron M. Inter-annual trend of the primary
751   contribution of ship emissions to PM 2.5 concentrations in Venice (Italy): Efficiency of emissions mitigation
752   strategies. Atmos Environ 2015;102:183-190.
753 Cristofanelli P, Bonasoni P, Carboni G, Calzolari F, Casarola L, Sajani SZ, Santaguida R. Anomalous high ozone
754   concentrations recorded at a high mountain station in Italy in summer 2003. Atmos Environ
755   2007;41(7):1383-1394.
756 Cuevas A. A partial overview of the theory of statistics with functional data. J. Stat. Plan. Inference 2014;147:1-23.
757 Curci G, Beekmann M, Vautard R, Smiatek G, Steinbrecher R, Theloke J, Friedrich R. Modelling study of the impact of
758   isoprene and terpene biogenic emissions on European ozone levels. Atmos Environ 2009;43(7):1444-1455.
759 Cyrys J, Eeftens M, Heinrich J, Ampe C, Armengaud A, Beelen R, et al.Variation of NO2 and NOx concentrations
760   between and within 36 European study areas: results from the ESCAPE study. Atmos Environ 2012;62:374-
761   390.
762 Demšar J. Statistical comparisons of classifiers over multiple data sets. J Mach Learn Res 2006;7:1-30.
763 Di Giuseppe F, Riccio A, Caporaso L, Bonafe G, Gobbi GP, Angelini F. Automatic detection of atmospheric boundary
764   layer height using ceilometers backscatter data assisted by a boundary layer model. Q J R Meteorol Soc
765   2012;138:649-663.
766 Duane M, Poma B, Rembges D, Astorga C, Larsen BR. Isoprene and its degradation products as strong ozone
767   precursors in Insubria, Northern Italy. Atmos Environ 2002;36(24):3867-3879.
768 EEA (European Environment Agency). AirBased The European Air Quality Database.
769   http://www.eea.europa.eu/themes/air/air-quality/map/airbase, 2016 (accessed February 2016).
770 Gentner DR, Worton DR, Isaacman G, Davis LC, Dallmann TR, Wood EC, et al. Chemical composition of gas-phase
771   organic carbon emissions from motor vehicles and implications for ozone production. Environ Sci Technol
772   2013;47(20):11837-11848.
773 Grice, S., Stedman, J., Kent, A., Hobson, M., Norris, J., Abbott, J., Cooke, S.. Recent trends and projections of primary
774   NO2 emissions in Europe. Atmos.Environ. 2009;43:2154-2167.
775 JRC- AQUILA. Position Paper - Assessment on siting criteria, classification and representativeness of air quality
776   monitoring stations. Available at: http://ec.europa.eu/environment/air/pdf/SCREAM%20final.pdf [last
777   accessed: April 2016]
778 Kaiser A. Origin of polluted air masses in the Alps. An overview and first results for MONARPOP. Environ Pollut
779   2009;157(12):3232-3237.
780 Keuken MP, Roemer MGM, Zandveld P, Verbeek RP, Velders GJM. Trends in primary NO 2 and exhaust PM
781   emissions from road traffic for the period 2000–2020 and implications for air quality and health in the
782   Netherlands. Atmos Environ 2012;54:313-319.
783 Khan MB, Masiol M, Formenton G, Di Gilio A, de Gennaro G, Agostinelli C, Pavoni B. Carbonaceous PM2.5 and
784   secondary organic aerosol across the Veneto region (NE Italy). Sci Total Environ 2016;542:172-181.
785 Kley D, Kleinmann M, Sanderman H, Krupa S. Photochemical oxidants: state of the science. Environ Pollut
786   1999;100:19-42.
787 Kurtenbach R, Kleffmann J, Niedojadlo A, Wiesen P. Primary NO2 emissions and their impact on air quality in traffic
788   environments in Germany. Environ Sci Europe 2012;24(12):1-8.
789 ISPRA, Italian Institute for Environmental Protection and Research. Disaggregated emission inventory.
790   http://www.sinanet.isprambiente.it/it/inventaria/ disaggregazione-dellinventario-nazionale-2010, 2015
791   (accessed 30 October 2015).
792 Lenschow, P., Abraham, H.-J., Kutzner, K., Lutz, M., Preuß, J.-D.,, Reichenbacher, W. Some ideas about the sources of
793   PM10. Atmos Environ 2001;35:S23–S33.
794 Li J, Cuesta-Albertos JA, Liu RY. DD-classifier: Nonparametric classification procedures based on DD-plot. J Am Stat
795   Assoc 2012;107:737–753.
796 Liu RY. On a Notion of Data Depth Based on Random Simplices. The Annals of Statistics 1990;18(1):405-414.

797 Lopez-Pintado S, and Romo J. On the Concept of Depth for Functional Data. Journal of the American Statistical
798   Association 2009;104(486):718–734.
799 Lopez-Pintado S, and Romo, J. A half-region depth for functional data. Computational Statistics and Data Analysis
800   2011;55(4):1679–1695.
801 Masiol, M., Centanni, E., Squizzato, S., Hofer, A., Pecorari, E., Rampazzo, G., Pavoni, B. GC-MS analyses and
802   chemometric processing to discriminate the local and long-distance sources of PAHs associated to
803   atmospheric PM2.5. Environ. Sci. Pollut. Res. 2012;19(8):3142-3151.
804 Masiol M, Formenton G, Pasqualetto A, Pavoni B. Seasonal trends and spatial variations of PM10-bounded polycyclic
805   aromatic hydrocarbons in Veneto Region, Northeast Italy. Atmos Environ 2013;79:811-821.
806 Masiol M, Formenton G, Giraldo G, Pasqualetto A, Tieppo P, Pavoni B. The dark side of the tradition: the polluting
807   effect of Epiphany folk fires in the eastern Po Valley (Italy). Sci Total Environ 2014a;473-474: 549-564.
808 Masiol, M., Squizzato, S., Rampazzo, G., Pavoni, B. Source apportionment of PM2.5 at multiple sites in Venice (Italy):
809   Spatial variability and the role of weather. Atmos. Environ. 2014b;98:78-88.
810 Masiol M, Agostinelli C, Formenton G, Tarabotti E, Pavoni B. Thirteen years of air pollution hourly monitoring in a
811   large city: Potential sources, trends, cycles and effects of car-free days. Sci Total Environ 2014c;494–
812   495:84–96.
813 Masiol M, Benetello F, Harrison RM, Formenton G, De Gasperi F, Pavoni B. Spatial, seasonal trends and
814   transboundary transport of PM2.5 inorganic ions in the Veneto Region (Northeastern Italy). Atmos Environ
815   2015;117:19–31.
816 Mosler K, Polyakova Y. General notions of depth for functional data. arXiv 2012; arXiv:1208.1981.
817 Munir S, Chen H, Ropkins K. Modelling the impact of road traffic on ground level ozone concentration using a quantile
818   regression approach. Atmos Environ 2012;60:283-291.
819 Pohlert, T. PMCMR: Calculate Pairwise Multiple Comparisons of Mean Rank Sums. R package version 1.3.
820   http://CRAN.R-project.org/package=PMCMR, 2015.
821
822 Putaud JP, Raes F, van Dingenen R, Brüggemann E, Facchini M C, Decesari S, et al. A European aerosol
823   phenomenology – 2: chemical characteristics of particulate matter at kerbside, urban, rural and background
824   sites in Europe. Atmos Environ 2004;38:2579–2595.
825 Putaud, JP, Van Dingenen R, Alastuey A, Bauer H, Birmili W, Cyrys J, et al. A European aerosol phenomenology – 3:
826   Physical and chemical characteristics of particulate matter from 60 rural, urban, and kerbside sites across
827   Europe. Atmos Environ 2010;44:1308–1320.
828 R Core Team. R: A language and environment for statistical computing. R Foundation for Statistical Computing,
829   Vienna, Austria, 2016. URL https://www.R-project.org/.
830 Ramsay JO, Silverman BW. Functional Data Analysis. Springer, 2006.
831 Romano, B., Zullo, F. Half a century of urbanization in southern European lowlands: a study on the Po Valley
832   (Northern Italy). Urban Res. Practice 2015; 8:1-22.
833 Seibert P, Feldmann H, Neininger B, Bäumle M, Trickl T. South foehn and ozone in the Eastern Alps–case study and
834   climatological aspects. Atmos Environ 2009;34(9):1379-1394.
835 Sen PK. Estimates of the regression coefficient based on Kendall's tau. J Am Stat Assoc 1968;63:1379-1389.
836 Squizzato, S., Masiol, M., Visin, F., Canal, A., Rampazzo, G., Pavoni, B. The PM2.5 chemical composition in an
837   industrial zone included in a large urban settlement: main sources and local background. Environ. Sci.
838   Process. Impacts 2014;16:1913-1922.
839 Theil H. A rank-invariant method of linear and polynomial regression analysis. In: Henri Theil's Contributions to
840   Economics and Econometrics. Springer, Netherlands, pp. 345-381; 1992.
841 Vecchi R, Valli G. Ozone assessment in the southern part of the Alps. Atmos Environ 1998; 33(1):97-109.
842 Vecchi R, Valli G, Fermo P, D'Alessandro A, Piazzalunga A, Bernardoni V. Organic and inorganic sampling artefacts
843   assessment. Atmos Environ 2009;43:1713-1720.
844 Vingarzan R. A review of surface ozone background levels and trends. Atmos Environ 2004; 38: 3431-3442.
845 Wotawa G, Kröger H, Stohl A. Transport of ozone towards the Alps–results from trajectory analyses and photochemical
846   model studies. Atmos Environ 2000;34(9):1367-1377.
847 WHO (World Health Organization). Air Quality Guidelines for Europe. European Series No 91,World Health
848   Organization. WHO Regional Publications, Geneva; 2000.
849 Zhu, T., Melamed, M., Parrish, D., Gauss, M., Klenner, L.G., Lawrence, M., Konare, A. Liousse, C., 2012. Impacts of
850   Megacities on Air Pollution and Climate. WMO, Geneva.
851 Zuo Y, Serfling, RJ. General notions of statistical depth function. The Annals of Statistics 2000;28(2):461-482.

Table 1. Characteristics of the sampling sites and analysed pollutants. Municipality refers to the territorial district where the sampling site is located: if the site is not located in the main town of a municipality, the city/town is given in brackets.

Province	No.	Code	Lat.	Long.	Height (m)	Municipality (City/Town)	Site full name	Area type	Monitored pollutants
BL	1	**BL.RUR1**	46.339	11.802	2020	Falcade	Passo Valles	Rural background	NOx, O3
	2	**BL.RUR2**	46.163	12.361	615	Pieve d'Alpago	Pieve d'Alpago	Rural background	NOx, O3, SO2, PM10,
	3	**BL.SUB**	46.031	11.906	263	Feltre	Area Feltrina	Suburban	CO, NOx, O3, SO2, PM10
	4	**BL.URB**	46.144	12.219	401	Belluno	BL-città	Urban background	CO, NOx, O3, SO2, PM10
TV	5	**TV.RUR**	45.837	12.51	14	Treviso (Mansuè)	Mansuè	Rural background	CO, NOx, O3 PM10
	6	**TV.URB1**	45.672	12.238	15	Treviso	TV-Via Lancieri	Urban background	CO, NOx, O3, SO2, PM10, PM2.5
	7	**TV.URB2**	45.89	12.307	72	Conegliano	Conegliano	Urban background	CO, NOx, O3, SO2, PM10
VI	8	**VI.RUR**	45.849	11.569	1366	Asiago	Asiago-Cima Ekar	Rural background	NOx, O3
	9	**VI.URB4**	45.759	11.736	114	Bassano	Bassano del Grappa	Urban background	NOx, O3 PM10
	10	**VI.URB1**	45.56	11.539	36	Vicenza	VI-Quartiere Italia	Urban background	CO, NOx, O3
	11	**VI.URB2**	45.532	11.522	33	Vicenza	VI-Ferrovieri	Urban background	CO, NOx, O3, SO2
	12	**VI.URB3**	45.714	11.368	190	Schio	Schio-via Vecellio	Urban background	NOx, O3 PM10, PM2.5
	13	**VI.TRA**	45.545	11.533	35	Vicenza	VI-San Felice	Urban-traffic	CO, NOx SO2, PM10
	14	**VI.IND1**	45.536	11.294	154	Chiampo	Chiampo	Urban-industrial	NOx
	15	**VI.IND2**	45.465	11.386	61	Montebello Vicentino	Montebello Vicentino	Suburban-Industrial	NOx
VR	16	**VR.RUR**	45.589	11.037	824	Boscochiesanuova	Boscochiesanuova	Rural background	CO, NOx, O3, SO2, PM10
	17	**VR.SUB**	45.462	10.911	91	Verona (Cason del Chievo)	VR-Cason	Suburban	CO, NOx, O3, SO2, PM10, PM2.5
	18	**VR.URB1**	45.443	11.007	64	Verona	VR-Piazza Bernardi	Urban background	CO, NOx
	19	**VR.URB2**	45.399	11.285	30	Verona (San Bonifacio)	San Bonifacio	Urban background	CO, NOx, O3, SO2, PM10, PM2.5
	20	**VR.URB3**	45.183	11.311	25	Legnago	Legnago	Urban background	NOx, O3 PM10
	21	**VR.TRA1**	45.444	10.963	62	Verona	VR-Borgo Milano	Urban-traffic	CO, NOx SO2, PM10
	22	**VR.TRA2**	45.41	10.989	60	Verona	VR-San Giacomo	Urban-traffic	CO, NOx SO2
	23	**VR.TRA3**	45.416	10.969	65	Verona	VR-ZAI	Urban-traffic	CO, NOx, O3, SO2
	24	**VR.IND**	45.543	10.886	183	Fumane	Fumane	Industrial	NOx SO2, PM10,
VE	25	**VE.RUR**	45.694	12.786	5	Concordia Sagittaria	Concordia Sagittaria	Rural background	NOx, O3
	26	**VE.URB1**	45.428	12.313	1	Venezia	VE-Sacca Fisola	Urban background	NOx, O3, SO2, PM10
	27	**VE.URB2**	45.5	12.261	1	Venezia (Mestre)	VE-Parco Bissuola	Urban background	CO, NOx, O3, SO2, PM10
	28	**VE.URB3**	45.629	12.59	3	San Donà di Piave	San Donà di Piave	Urban background	CO, NOx, O3 PM10, PM2.5

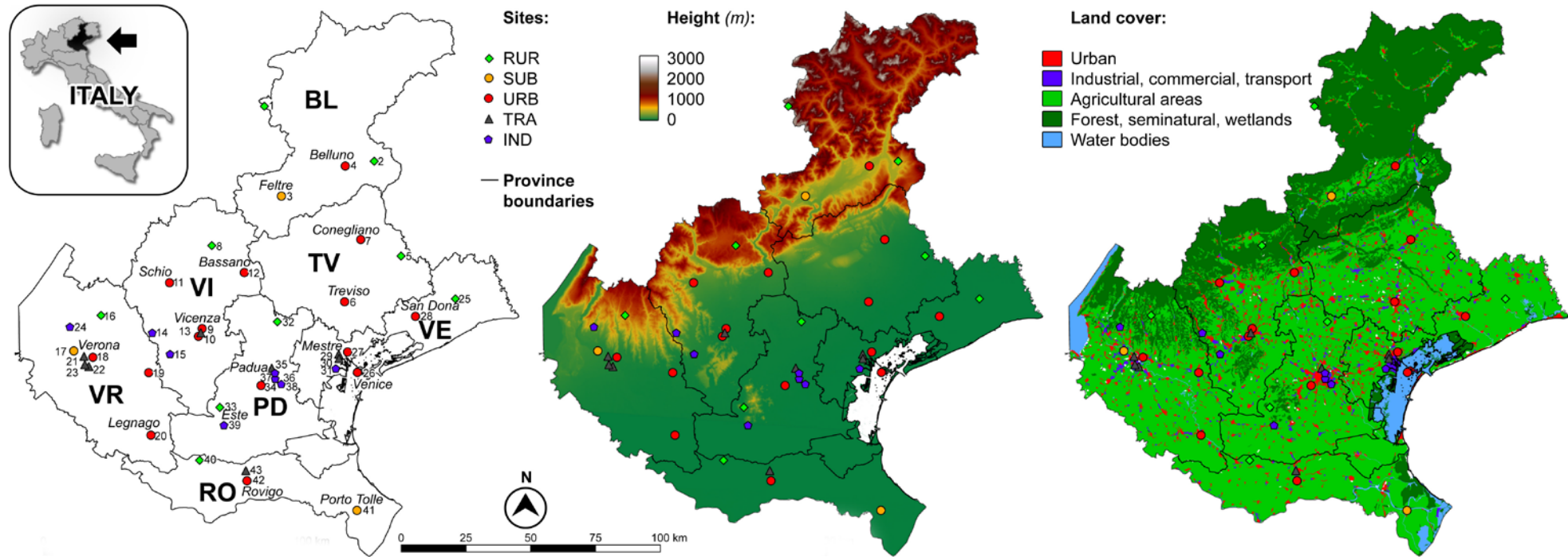|								
	29	**VE.TRA1**	45.49	12.218	2	Venezia (Mestre)	VE-Via Tagliamento	Urban-traffic	CO, NOx SO2, PM10
	30	**VE.TRA2**	45.474	12.22	2	Venezia (Marghera)	VE-Via Beccaria	Urban-traffic	CO, NOx , PM10
	31	**VE.IND**	45.438	12.205	2	Venezia (Marghera)	VE-Malcontenta	Industrial	CO, NOx SO2
PD	32	**PD.RUR1**	45.594	11.909	24	Santa Giustina in Colle	S. Giustina in Colle	Rural background	CO, NOx, O3
	33	**PD.RUR2**	45.289	11.642	18	Padova (Cinto Euganeo)	Parco Colli Euganei	Rural background	NOx, O3, SO2, PM10
	34	**PD.URB**	45.371	11.841	13	Padova	PD-Mandria	Urban background	CO, NOx, O3, SO2, PM10
	35	**PD.TRA**	45.433	11.89	11	Padova	PD-Arcella	Urban-traffic	CO, NOx, O3, SO2, PM10
	36	**PD.IND1**	45.395	11.909	10	Padova	PD-APS-1-Ignoto	Urban-industrial	CO, NOx, O3, SO2, PM10, PM2.5
	37	**PD.IND2**	45.415	11.907	10	Padova	PD-APS-2-Carli	Urban-industrial	CO, NOx, O3, SO2, PM10, PM2.5
	38	**PD.IND3**	45.378	11.94	8	Padova	PD-Granze	Urban-industrial	PM10
	39	**PD.IND4**	45.227	11.666	12	Este	Este	Suburban-Industrial	CO, NOx, O3, SO2, PM10
RO	40	**RO.RUR**	45.103	11.554	8	Badia Polesine	Polesine-Villafora	Rural background	CO, NOx, O3, SO2
	41	**RO.SUB**	44.95	12.333	1	Porto Tolle	Porto Tolle	Suburban	NOx SO2, PM10, PM2.5
	42	**RO.URB**	45.039	11.79	3	Rovigo	RO-Borsea	Urban background	CO, NOx, O3, SO2
	43	**RO.TRA**	45.074	11.782	7	Rovigo	RO-Centro	Urban-traffic	CO, NOx, O3, SO2, PM10

855

856

857

858

859

860

861

862

863

864

865

866

867
868
869 **Figure 1.** Map of the Veneto Region: administrative (left); terrain relief (centre); land use and cover from CORINE Land Cover 2006 data (right).
870 Sampling sites are also represented as diamonds (RUR sites), dots (SUB and URB sites), triangles (TRA sites) and pentagons (IND sites).
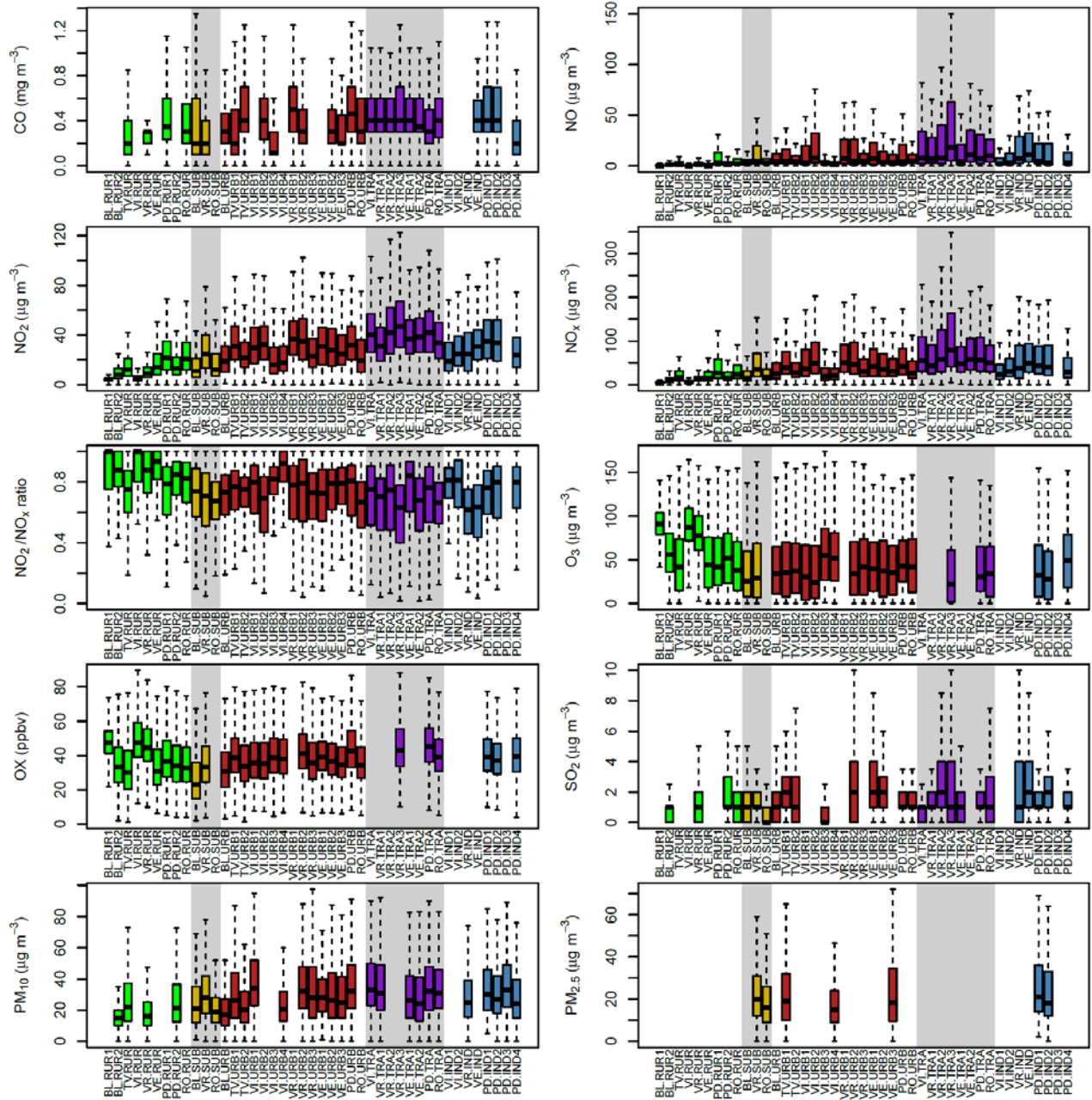
33

Figure 2. Average and ranges of concentrations of the analyzed pollutants as boxplots of raw data (line= median, box= inter-quartile range, whiskers= ±1.5*inter-quartile range). Sites are clustered following their categorisation.

Figure 3. Classification of the stations based DD-plot for nitrogen oxides. The analysis is based on multivariate functional simplicial data depth using nitrogen oxides (NO, NO_2 and NO_x).
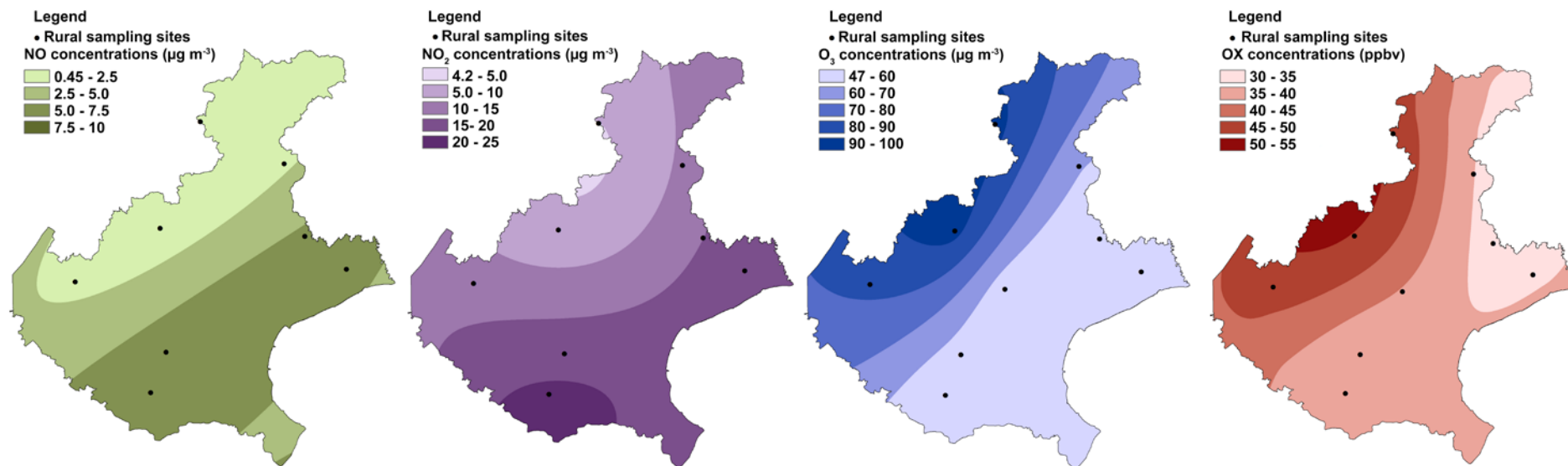
Figure 4. Maps of concentrations for NO, NO$_2$, O$_3$ and OX measured at the RUR sites. All RUR sites were used to interpolate data for O$_3$ and OX, while PD-RUR1 was not used for NO and NO$_2$ because of the anomalously high levels recorded. Ordinary kriging method was used for interpolation. Maps showing the standard errors associated with predictions are shown as Figure SI5.
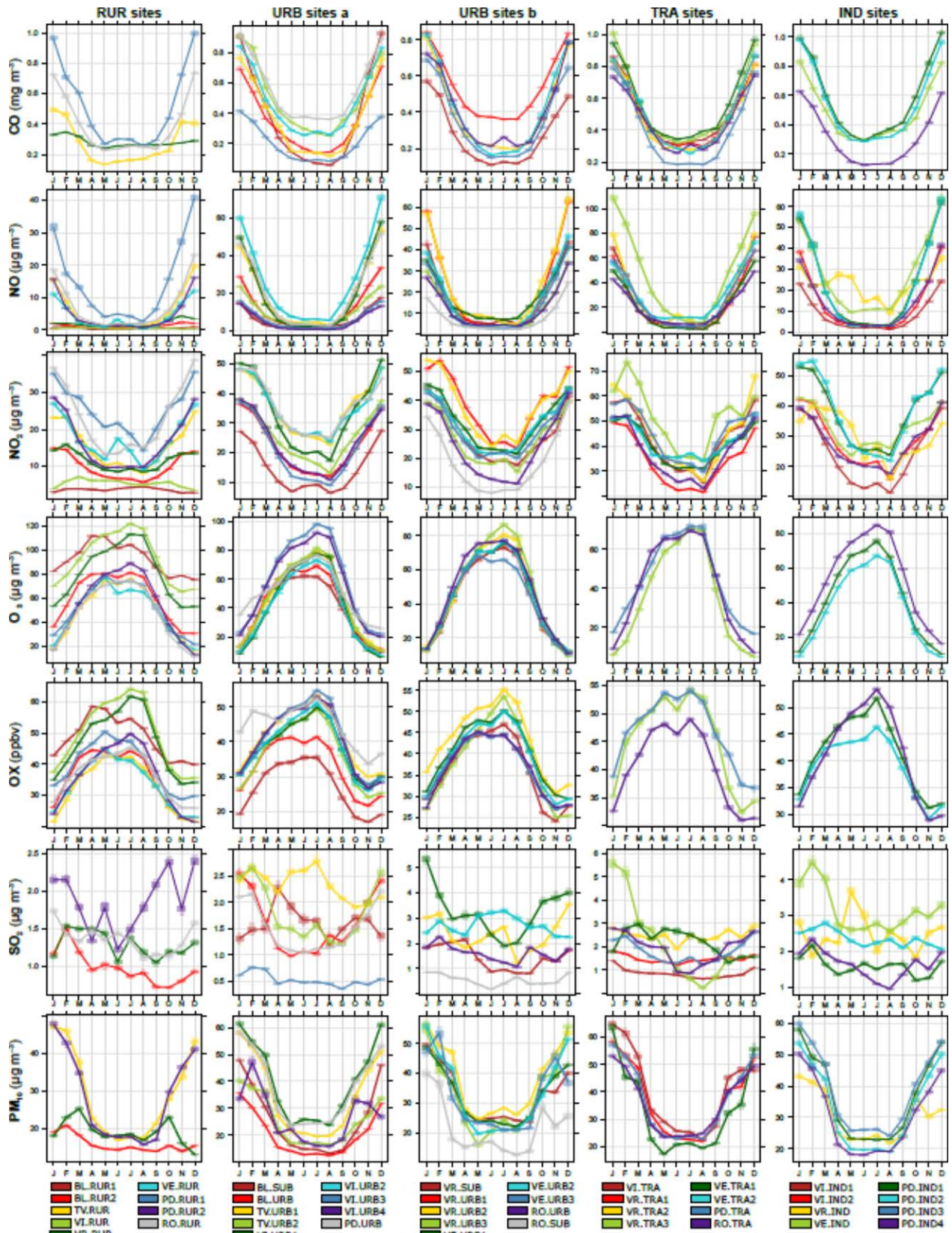
Figure 5. Seasonal variations of the monitored pollutants. Each plot reports the monthly average levels as a filled line and the associated 75th and 99th confidence intervals calculated by bootstrapping the data (n=200).
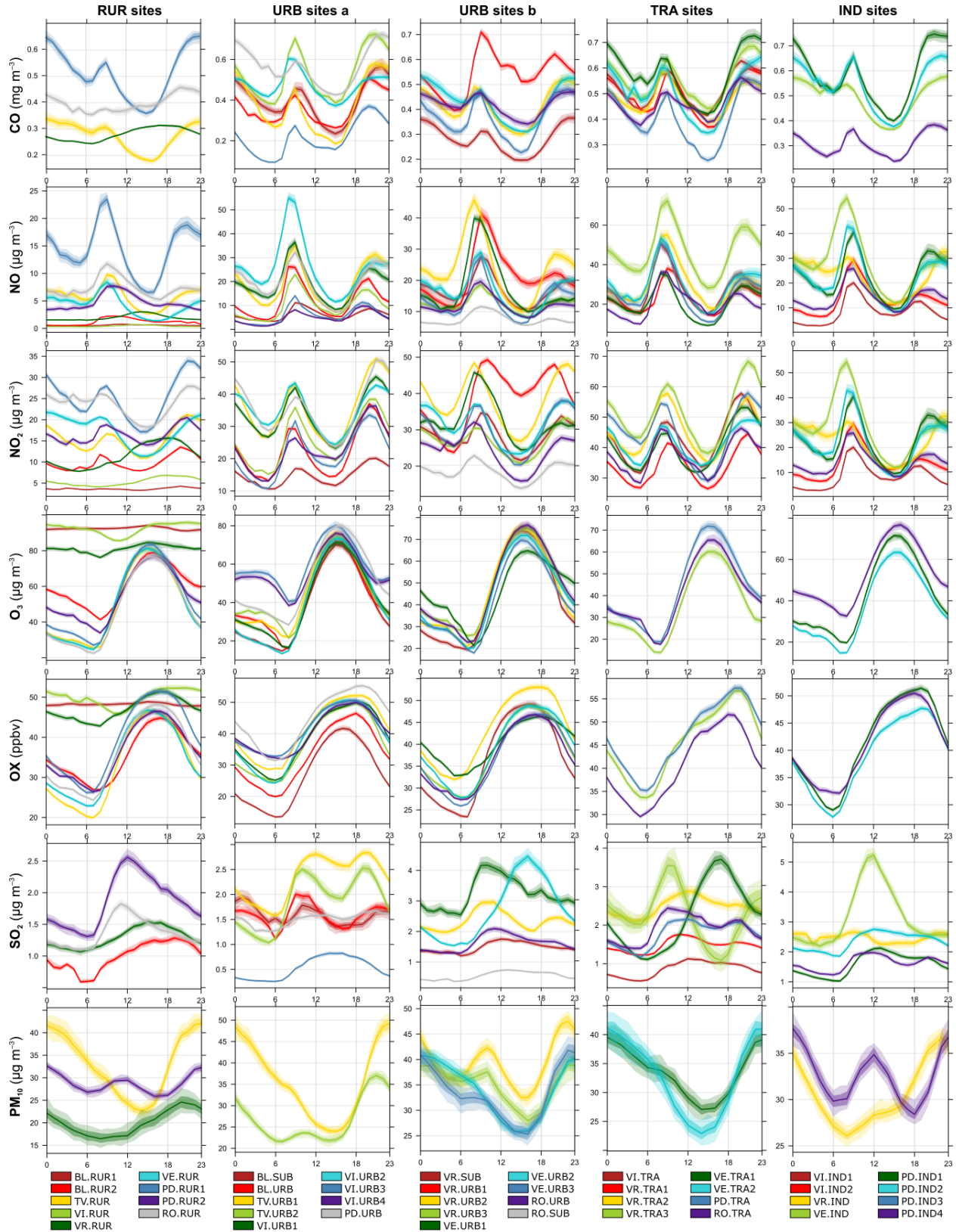
Figure 6. Diurnal variations of levels of measured pollutants computed over the hourly averaged data during the sampling period. Each plot reports the average level as a filled line and the associated 75th and 99th confidence intervals calculated by bootstrapping the data (n=200). Data are corrected for DST.
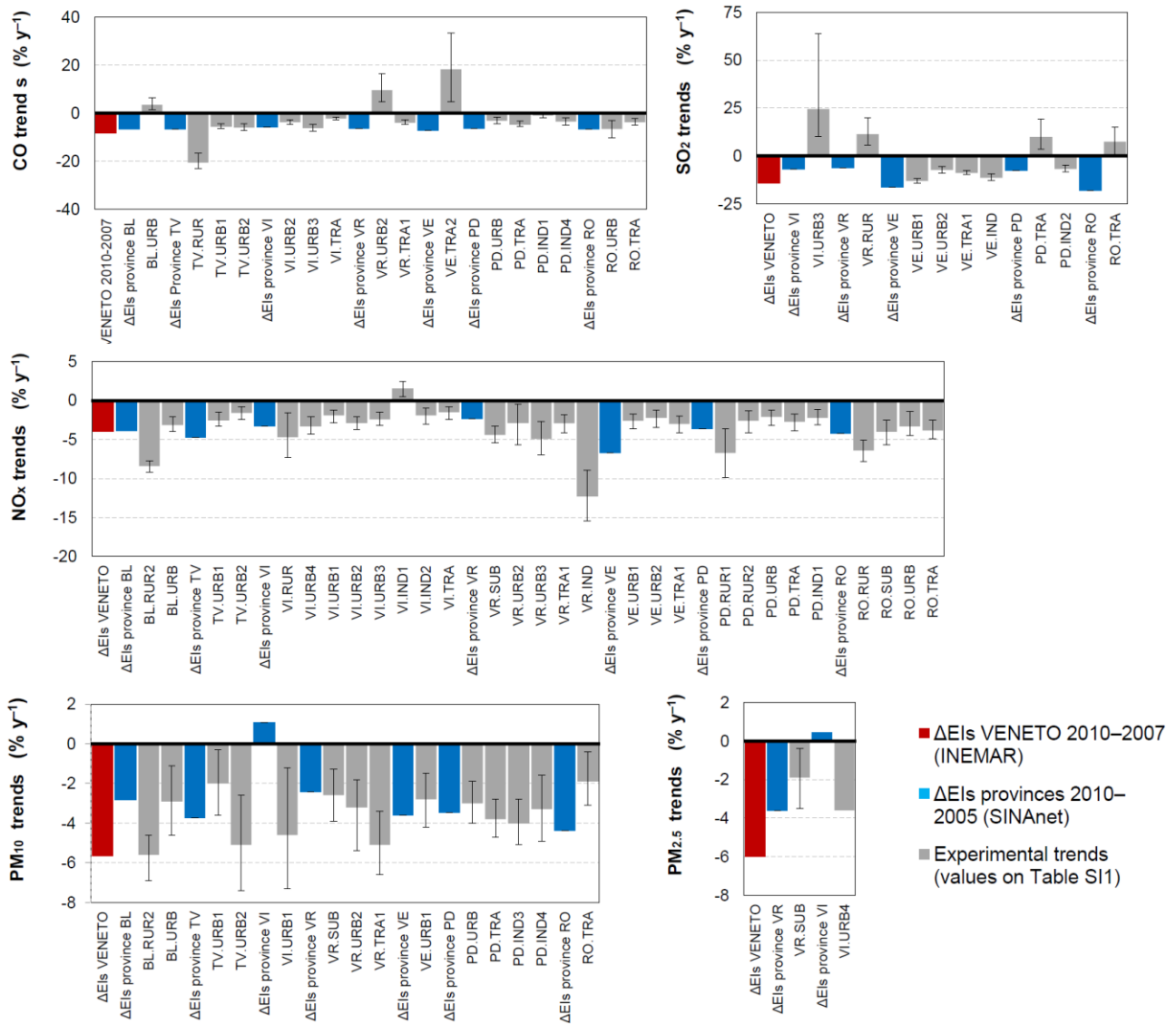
Figure 7. Results of the Theil-Sen analysis of trends (grey bars). The estimated trends are expressed as percentage; the confidence intervals of trends are given by error bars. Only sites showing significant trends (p-values < 0.05) are shown. The percentages of change in emissions provided by the most recent emission inventories are also provided and expressed as % y^{-1}: changes of EIs for the whole Veneto region (Δ_Veneto, red bars) refers to the difference of EIs between 2010 and 2007; changes of EIs for each province (Δ_BL, Δ_TV, Δ_VI , Δ_VR, Δ_VE, Δ_PD, Δ_RO, blue bars) refers to the difference of EIs between 2010 and 2005.